Advances in Reliability, Safety and Security, Part 9 – Kołowrocki, Dąbrowska (eds.)
© 2024 Polish Safety and Reliability Association, Gdynia, ISBN 978-83-68136-21-0 (printed), ISBN 978-83-68136-08-1 (electronic)

Advances in Reliability, Safety and Security
ESREL 2024
Monograph Book Series

System Reliability Assessment Of Component-Integrated Wireless Sensor Networks With Consideration Of Data Accuracy

Sören Meyer zu Westerhausen, Gurubaran Raveendran, Daniel Rosemann,
Johanna Wurst, Roland Lachmayer

Institute forProduct Development, Leibniz University Hannover, An der Universität 1, 30165 Hannover, Germany

---

Abstract

The system reliability of wireless sensor networks (WSN) is an important issue to ensure robust data acquisition. Especially when sensor networks are directly integrated into components, for example inside the composite layup of composite parts, the non-repairability has to be considered for sensor placement. Since the quality of the acquired data is as important as the reliability of the network itself to fulfill the main function of data acquisition, a combined perspective on data and hardware is needed. Therefore, an algorithmic approach for data path-based reliability assessment is enhanced to the estimation of data accuracy regarding signal quality losses during transmission. This approach uses signal attenuation along data paths to estimate changes in the Signal-to-Noise ratio (SNR) and therefore in the accuracy of acquired data. To demonstrate the algorithmic effectiveness, a case study is presented that analyzes an exemplary WSN from both a data and a hardware perspective. Resulting from the demonstrated effectiveness and applicability, the approach presented in this paper aids engineers in designing WSNs for reliable data acquisition.

Keywords: system reliability; wireless sensor networks; hardware lifetime; data accuracy

---

1. Introduction

During the last decades, a trend of smart products toward the application of sensors could be observed. This trend of digitalization, enabling for example topics like digital twins, could be observed in different fields of mechanical engineering. The integration of sensors into machine components allows to measure more robustly since the sensors are less influenced by environmental factors (Welzbacher et al., 2023). Regarding structural components, for example, made of composite materials for airplanes or wind turbines, sensors inside the material could be used for damage detection (Damm et al., 2020). Furthermore, the acquired data could be used to optimize structural components from one generation to the next in a process of technical inheritance (Lachmayer et al., 2014; Lachmayer et al., 2016).

Considering large-scale components, sensor networks are needed to allow area-wide monitoring. Especially wireless sensor networks (WSNs) allow to reduce components weight compared to wired sensor networks (Lee et al., 2009). Therefore, the sensor network consists of so-called sensor nodes, where data is acquired with the sensors, processed and stored by a microcontroller, and transmitted by a transceiver afterwards. Depending on the transmission protocol, the data is either sent hop-by-hop from one sensor node to the next or directly to the sink node, where the data of the different sensor nodes in the network is collected before it is further transmitted to the user (Akyildiz et al., 2002).

An exemplary WSN with the structure of a sensor node is shown in Figure 1. In the depicted case, an airplane wing is monitored regarding the loads in the form of strains by a WSN. The data is transmitted by the so-called FLOODING protocol from one sensor node to the next until it arrives at the sink node at the wing root. Therefore, the data is sent along a data path, which usually is the shortest path. Each sensor node in the network consists of a strain gauge, an Analog-Digital-Converter (A/D-converter), a microprocessor with integrated transceiver, and a battery.

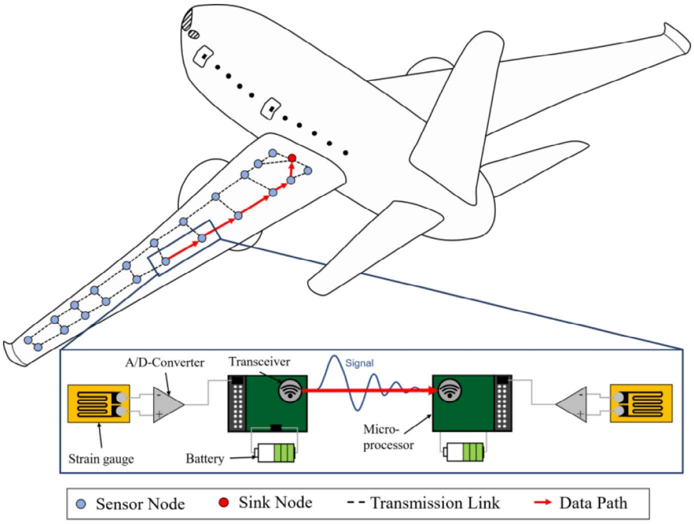

Fig. 1. Exemplary WSN on an airplane wing with sensor nodes consisting of strain gauges, A/D-converters and microprocessors with transceiver for data transmission with the problem of signal attenuation.

However, as one can see in Figure 1, the position of the sensor nodes brings two different challenges regarding the network reliability analysis, apart from the limited lifetime due to the battery by the energy consumption of each node:

1. Data transmitted from nodes far away from the sink node might suffer from signal attenuation and therefore reduced accuracy due to higher transmission distances and
2. Sensor nodes at positions of higher loads, for example due to bending of the wing, have a decreased lifetime in comparison to nodes at less loaded positions.

To take both challenges into account when analysing the system reliability of a WSN, a new approach is presented in the following. Therefore, the paper is organised as follows. Section 2 gives an overview of related works on the topic of data accuracy and system reliability of WSNs. Based on these related works, an approach is presented on how to take the measurement accuracy into account while analysing the system reliability of a WSN is presented in Section 3. To show its applicability, it is applied in a case study, which is described in Section 4. Last, Section 5 summarizes the results of this paper and gives an outlook on future research.

2. Related Works

In the literature, different works with a different focus on the reliability of sensor networks can be found. The literature review of Meyer zu Westerhausen et al. showed that most works on this topic have a combination of hardware and a data perspective on the reliability of sensor networks data acquisition task. Most of the approaches described in this paper use Markov chains or matrix systems as models for data paths in the reliability assessment (Meyer zu Westerhausen et al., 2023b). For example, (Ibrahim et al., 2019) uses Markov chains to estimate the availability of a sensor network regarding the battery lifetime as the main issue to take into account for repairs. To gain a better understanding of the impact of different operation scenarios of sensor nodes in the modes “active” and “sleep”, the work of (Wang et al., 2014) presents a study on the reliability of sensor nodes in three operation scenarios and the corresponding lifetime due to energy consumption. However, the works using these methods focus on repairable systems, which is not possible when component-integrated sensor networks are considered. Regarding this topic, reliability block diagrams (RBD) and fault tree analysis (FTA) can be considered as methods for system reliability assessment.

The work of (Wang et al., 2021) addresses the reliability analysis of a WSN with a dynamic FTA. The reason for using this method is the consideration of different backup strategies, like for example the use of a WSN with hot and cold backup of sensor nodes. Another approach is presented by (Lin et al., 2010), who uses an RBD for the reliability analysis of a WSN. In this paper, a WSN is assumed as a graph $G = (V, E)$, consisting of nodes V and edges E. In the case of a WSN, the edges are formed by links for data transmission, resulting from the chosen transmission protocol. To calculate the networks system reliability, the network is divided by a division algorithm into subgraphs, which form a star topology. In this case, all links of the subgraph are connected to only one node. Therefore, the system reliability of each subgraph is calculated with a series ordered RBD of all sensor nodes and links (see equation (1)).

$$R_G(t) = \prod_{i=1}^{n} R_{G,i}(t) \cdot \prod_{i=1}^{n} R_{E_{p,i}}(t) \tag{1}$$

However, this approach has the disadvantage that it is not possible to analyse each data path in the WSN separately, to find possible issues and optimization potentials when the system reliability does not fit the requirements for the product. Considering this issue of this methodology, another alternative is presented by (Dâmaso et al., 2014). In this work, each data path of a WSN is modeled for reliability analysis, using an RBD. Therefore, it is assumed that data is transmitted from each sensor node only along the shortest data path from the transmitting sensor node, until it arrives at the sink node. The data paths are therefore forming a series order of all the sensor nodes and links along the path. After the data paths of each sensor node in the WSN are modeled like this, it is analysed if some sensor nodes form a region together, which is an area where the same physical phenomenon is measured. Therefore, it is assumed, that sensor nodes inside the same region measure redundantly. As a result, the RBDs of the sensor nodes data paths are combined into a region model. The approach of (Dâmaso et al., 2014) has the advantage of making reliability analysis of the WSN very transparent, and therefore, possible weaknesses regarding the reliability of the whole WSN in the network could be identified easily. On the other hand, the reliability analysis stops at the region level and does not consider the system reliability of the whole WSN. Furthermore, the methodology presented by (Dâmaso et al., 2014) only considers energy consumption as a reliability criterion.

To enhance the method of Dâmaso et al., the study of (Meyer zu Westerhausen et al., 2023a) presents an approach, where the region analysis is performed on the example of a WSN for strain measurements inside a composite part. In this approach, a region is formed when two or more sensor nodes are close to one another and measure similar strains. This is the case, when the strain measurements differ only as much as the measuring tolerance of the sensor could not distinguish. If sensor nodes are not forming regions together with other regions, they are considered as a region only by consisting of themselves and their data path. After the affiliation of each sensor node to a region is checked, the regions are combined in a series order as an RBD of the whole WSN. In the presented approach, this is due to the fact that the sensor node is assumed to be needed for the measuring task and therefore, the whole WSN would fail its main function in case of a failing region. In the presented study, this approach was implemented into a Matlab tool to allow an automatic assessment of the system reliability of a WSN for strain measuring applications. However, this approach is also only focussing on the hardware side of a WSNs system reliability as the beforementioned approaches.

Besides the hardware point of view on the system reliability, the review of (Meyer zu Westerhausen et al., 2023b) shows that data accuracy and data loss during transmission are mostly addressed, when it comes to consideration of data in terms of reliability in sensor networks. Since the focus of this paper is the consideration of signal quality changes and therefore the data accuracy, works on this topic are considered only in the following.

3. Integration of signal attenuation and data quality loss in the system reliability assessment

The methodology presented by (Meyer zu Westerhausen et al., 2023a) is taken as basis for the integration of measurement accuracy due to signal attenuation into the system reliability assessment of a WSN. Therefore, the methodology is enhanced regarding two different aspects, which are described in the following. First, an enhancement regarding the mechanical properties and system reliability calculations are described. Afterwards, the calculation of the accuracy due to signal attenuation is described.

3.1. Calculation of the mechanical system reliability

To calculate the mechanical system reliability, the reliability of each sensor node has to be analyzed first. In the approach presented here, a sensor node consists of one strain gauge as a sensor, an A/D-Converter, a microprocessor with integrated transceiver and the cables to connect these elements with each other (see Figure 1). Since all components are assumed to be non-repairable and a failure of one of these components would lead to a failure of the whole sensor node, they form a series order in an RBD. Therefore, the reliability of each sensor node is calculated as

$$R_{SensorNode}(t) = R_{StrainGauge}(t) \cdot R_{Cable}(t) \cdot R_{A/D-Converter}(t) \cdot R_{Cable}(t) \cdot R_{Microprocessor}(t). \tag{2}$$

Each components failure probability could be described with a two-parametric Weibull distribution. In the case of electric components, the shape parameter is often $b = 1$, which describes the failure probability in the form of an exponential distribution (Bertsche, 2008). However, sensors like strain gauges suffer from signal drifts and therefore measurement inaccuracies due to cyclic loads (Innocent et al., 2022; Keil, 2017). This leads to the assumption of a shape parameter $b > 1$, as it is typical for failures due to wear and fatigue. Since those fatigue failures in dependence on the applied load could be described by the Wöhler line with its slope factor k, the corresponding Weibull scale parameter T can be calculated for every strain amplitude the strain gauges of the WSN are facing at the different positions. The relationship between the Wöhler line and the failure probability described with the Weibull distribution is exemplary shown in Figure 2.

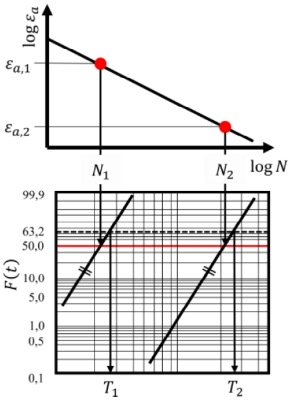

Fig. 2. Relationship of the Wohler line and the failure probability described by a Weibull distribution.

Since the Wöhler line describes a 50 % failure probability, each point of the line can be used to calculate T with the use of a known reference point on the Wohler line. The calculation is shown in (3), where the values with index '1' can be assumed as the reference values. This means, $\varepsilon_{a,1}$ is the strain amplitude applied and N_1 is the number of cycles, where failure occurs with 50 % probability with this strain amplitude.

$$T_2 = \frac{N_1 \cdot \left(\frac{\varepsilon_{a,1}}{\varepsilon_{a,2}}\right)^k}{\sqrt[b]{log\left(\frac{1}{0,5}\right)}}. \tag{3}$$

After the reliability of each sensor node as sub-system of a WSN is described as mentioned before, the reliability of the whole network has to be calculated. Therefore, the data paths in the network have to be analysed first. Assuming a DIRECT protocol is used where the data is transmitted from each sensor node to the sink node, the reliability of the data path could be described as a series order in an RBD and the data path's reliability could be described as

$$R_{DataPath}(t) = R_{SensorNode}(t) \cdot R_{Link}(t) \cdot R_{SinkNode}(t). \tag{4}$$

The term $R_{Link}(t)$ describes the reliability of the transmission link between the sensor node and the sink node. Since the sink node has only the function of gathering the data of all sensor nodes in a WSN to transmit it to the user, it only consists of a microprocessor with a transceiver. So, the reliability of the sink node equals the reliability of a microprocessor $R_{Microprocessor}(t)$. In case the FLOODING protocol is used, (4) would be enhanced by the reliability of all the sensor nodes and links, which transmit the data (Dâmaso et al., 2014).

After the RBD of each data path is build, the data paths of sensor nodes in common regions have to be combined as described in the methodology of (Meyer zu Westerhausen et al., 2023a). A region is defined here as an area of a component where the strains are so similar that they cannot be distinguished within the measurement tolerance of a strain gauge. Those regions could be identified based on FEM simulation data by comparison of strains from elements with neighboring elements. An in-house developed tool, programmed in Python and based on a region growing algorithm, is used for this purpose. To find sensor nodes in common regions, the node coordinates are compared to the coordinates of elements inside each region. If two or more sensor nodes are positioned in the same region, they measure redundantly and therefore form a parallel structure in an RBD. Therefore, when a DIRECT protocol is used, the region reliability would be calculated with (5).

$$R_{Region}(t) = R_{SinkNode}(t) \cdot \left[1 - \prod_{i=1}^{n}\left(1 - R_{SensorNode}(t) \cdot R_{Link}(t)\right)\right]. \quad (5)$$

In this equation, n is the number of redundant measuring nodes. Each sensor node forms a parallel with its link to the sink node, which is why the term is included in the term of the parallel ordered sensor nodes. However, since the data of all sensor nodes is gathered at the sink node, a failure would lead to the failure of the whole region because the measurements would no longer be transmitted to the end user. Therefore, the sink node's reliability is still handled as a serial element in the calculation.

When each region is modeled like this, the overall system reliability of the whole WSN can be calculated with an RBD of all regions in series order. Due to the fact of the design of the WSN, each sensor node is assumed to be needed for monitoring the component, and therefore a failure of one region would lead to a failure of the system.

3.2. Calculation of the measurement accuracy due to signal attenuation

Besides the calculation of the mechanical reliability of a WSN, the measurement accuracy has to be taken into account, too. If the data, that the user receives from the WSN, is inaccurate or incorrect, it might lead to false decisions. For example, when the data is used for calculations of the residual life of a component, a decision for too early replacement leads to unnecessary costs and a decision for too late replacement might lead to dangerous situations, when function relevant components are considered. Therefore, during the design phase of a WSN, the overall measurement accuracy has to be taken into account. To do so, the degradation of a signal due to environmental influences during transmission has to be taken into account.

For the calculation of accuracy changes during data transmission, the signal-to-noise ratio (SNR) is used in the methodology of this paper. The SNR defines the ratio between the power of a measured signal and the power of the background noise of the measurement system. For its calculation, the amplitudes of signal A_{Signal} and noise A_{Noise}, measured in volts or amperes, could be used. However, in some applications it might be useful to calculate the SNR in decibels, so (5) could be applied. This form of calculation of the SNR is used in the following, since it makes it easier to calculate the accuracy of measurements after transmission with consideration of signal attenuation.

$$\mathrm{SNR[dB]} = 10 \cdot \log_{10}\left[\left(\frac{A_{Signal}}{A_{Noise}}\right)^2\right]. \quad (6)$$

For the calculation of signal losses during transmission, the specific signal attenuation (in the following referred to as attenuation) is calculated in accordance to the recommendation ITU-R P.676-10 (09/2013) of the International Telecommunication Union (ITU, 2013). For the calculation, a mathematical model is used to consider signal intensity losses due to electromagnetic interactions of the signal's wave and the atmospheric gases (Giannetti et al., 2017). In this calculation, the environmental factors pressure, temperature and humidity as well as the distance between the point of transmission and the receiver and the frequency of the transmission have to be known (ITU, 2013). For the calculation of the attenuation, already defined functions, like the gaspl() function in Matlab, could be used.

After calculating the attenuation, the accuracy of the signal at the receiving point could be calculated. It is assumed that the signal intensity and therefore its amplitude decreases, but the noise amplitude of the measurement signal stays the same. This results in the calculation of the received signal amplitude as

$$A_{Signal,received} = A_{Signal,transmitted} - A_{attenuation}. \quad (7)$$

When the signals and the noise amplitude are known after transmission, the SNR at the receiving sensor node is calculated by replacing A_{Signal} in (6) with $A_{Signal,received}$ in (7). The comparison of the SNR at the beginning $(SNR_{Beginning})$ and the end (SNR_{End}) of the data transmission is then calculated as shown in (8). For the focus of this paper, this quotient is taken into further analysis of the WSN system reliability from the data perspective as accuracy metric. Therefore, the percentage error due to transmission $\%E_{Transmission}$ is calculated as

$$\%E_{Transmission} = 1 - \frac{SNR_{End}}{SNR_{Beginning}}. \quad (8)$$

4. Case study

To test the applicability of the proposed calculation methodology, an airplane aluminum wing box is used as a demonstrator, which is part of the airplane wing for its stiffness. The wing box, as shown in Figure 3, has a length of 15 m, which is based on the dimensions of a passenger aircraft, e.g. an Airbus A320. As a load-case, a displacement of w = *1'000 mm* is assumed at the free end of the wing box due to the lift of the wing. This load case is simulated using FEM in Abaqus CAE with Standard/Explicit Solver 2021. Therefore, the part itself is discretized using S4R shell elements with an edge length of ≈10 mm on a midsurface-model. Since in reality, the load-case would be carried out in a hall on a test bench, a temperature of 20 °C, 7.5 g/m³ vapor density and an air pressure of 1'013 hPa is assumed as environmental factors. Furthermore, the WSN is assumed to be built up as shown in Figure 3.

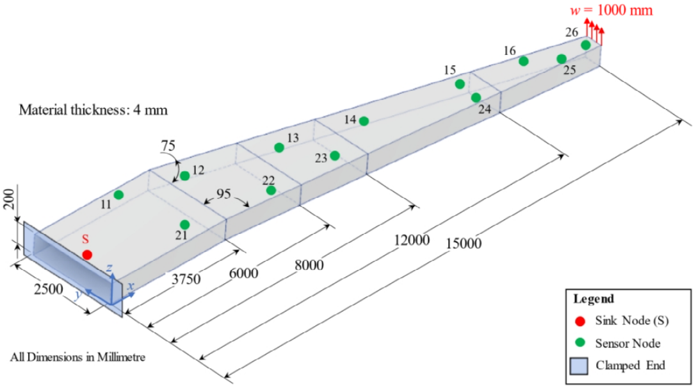

Node-Nr.	x [mm]	y [mm]	z [mm]
11	2319.08	2211.54	600.00
12	4385.81	1870.93	600.00
13	6047.55	841.68	600.00
14	8449.91	541.80	600.00
15	10949.87	432.26	600.00
16	12532.10	-99.55	600.00
21	2911.18	480.77	600.00
22	5559.72	92.45	600.00
23	7476.12	166.05	600.00
24	11149.87	-513.03	600.00
25	13596.58	-666.79	600.00
26	14854.55	-723.49	600.00
S	246.71	1250.00	600.00

Fig. 3. Draft of the wing box with the load case with a clamped end and a displacement at the free end for the case study.

As depicted in Figure 3, the WSN consists of 12 sensor nodes and one additional sink node. Each sensor node is built up by a strain gauge, an A/D-Converter and a microprocessor with integrated transceiver. The sensor nodes are aligned on two lines along the wing box for the purpose of shape sensing, as it is described by (Valoriani et al., 2022). Therefore, sensor nodes IDs along one line start with a '1' and along the other line with a '2'. Besides, the DIRECT protocol is used for data transmission, since the transmission range is comparatively low (max. 14.74 m). For the mechanical reliability analysis, the values for the parameters of a two-parametric Weibull distribution and Wöhler line shown in Table 1 are assumed. For the estimation of the Weibull shape parameter b, a strain amplitude of $\varepsilon = 0.9\,mm/m$ is used. Since the Weibull scale parameter T is not necessary for the calculation, it is not listed in Table 1. To perform the region analysis of the methodology described by (Meyer zu Westerhausen et al., 2023a), a tolerance of 1.5 % is assumed for strain gauge measurements, which is a typical value for strain gauges of the company HBM. Furthermore, the reliability of the links between the sensor nodes is assumed to be constantly $R_{Link}(t) = const. = 1$, as it was assumed by (Deif and Gadallah, 2017). Therefore, the wireless links would never fail. For the measurement accuracy, a noise amplitude $A_{Noise} = 0.00025\,dB$ is assumed, which allows to calculate the actual SNR of each sensor node based on the strains that could be derived from the FEM simulation.

Table 1. Parameters of the Weibull distribution and Wöhler line of each sensor node component for reliability analysis of the WSN.

Part	Shape Parameter b	Wöhler Slope Factor k
Strain gauge	2.0	8.0
A/D-Converter	2.3	10.0
Microprocessor with Transceiver	3.1	12.0
Cables	2.7	7.0

As a first step, the redundantly measuring sensor nodes are identified with use of the developed Python tool for region analysis. The results are shown in Figure 4. As one can see in Figure 4(b), the sensor nodes 13 and 23 are positioned in an area of the same color and therefore share a common region. Furthermore, one can see a finer segmentation of the elements to regions in the lower left corner of Figure 4(a). This is due to the fact that there is a higher difference of strain values from one element to the next at the part close to the clamped end. Since there are fewer differences regarding the strain values of each element in the middle of the component, the regions grow larger (Figures 4(b) and 4(c)). It could be observed in Figure 4(a) that the regions with a greater distance to the clamped end have a width of just one element, while the length could be eleven elements. This is because the strains differ along the x-axis of the component due to the stiffness differences between areas close to the corner and areas in the middle of the part. Besides, the excerpt d) of the region's plot show a higher segmentation of the regions at the free end. This results from the region analysis algorithm itself, since it takes the regions average strain value to decide if neighboring elements have similar strains and could be added to the region. Since the strains have very small values at the free end of the component, the percentage difference between the elements is too small to form common regions.

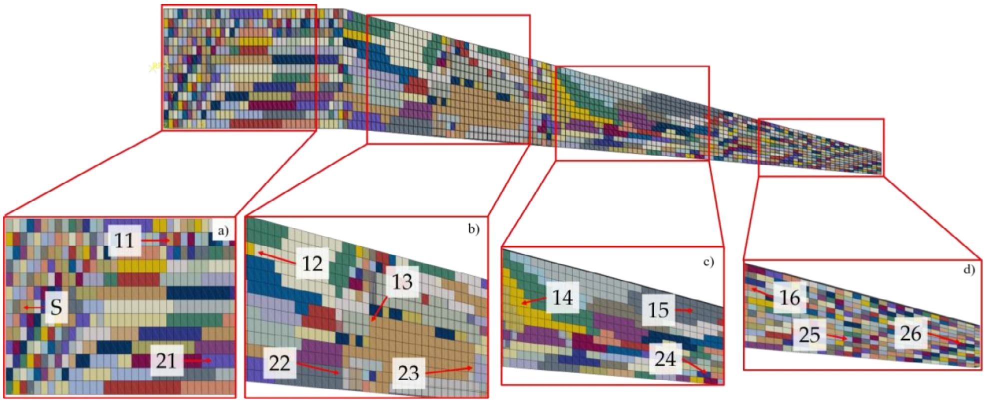

Fig. 4. Results of the region analysis for the strains in x-direction with a colored plot, showing each region as well as the marked positions of the sensor nodes at the corresponding elements in the FE model.

After the region analysis is performed and regions with redundantly measuring nodes are identified, the data paths are created and analyzed. Since in this case study, a data transmission with a DIRECT protocol is assumed, there are only data paths from each sensor node to the sink node. The data paths are formed as shortest paths, which length is calculated using the Euclidian distance. This path length is used to calculate the signal attenuation during transmission like it is described in Section 3.2. For this calculation, it is assumed to have a signal in decibels which is equal to the actual strain amplitude measured. The resulting SNR at the beginning and the end of the transmission as well as the percentage error as accuracy metric are shown in Figure 5(a).

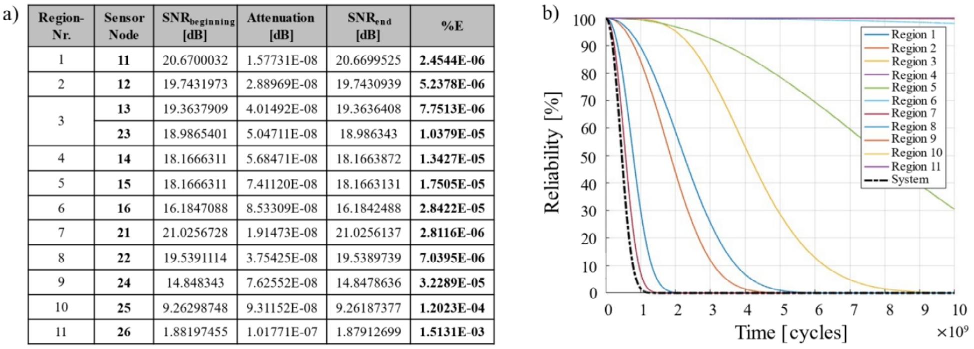
a)

Region-Nr.	Sensor Node	$SNR_{beginning}$ [dB]	Attenuation [dB]	SNR_{end} [dB]	%E
1	**11**	20.6700032	1.57731E-08	20.6699525	**2.4544E-06**
2	**12**	19.7431973	2.88969E-08	19.7430939	**5.2378E-06**
3	**13**	19.3637909	4.01492E-08	19.3636408	**7.7513E-06**
	23	18.9865401	5.04711E-08	18.986343	**1.0379E-05**
4	**14**	18.1666311	5.68471E-08	18.1663872	**1.3427E-05**
5	**15**	18.1666311	7.41120E-08	18.1663131	**1.7505E-05**
6	**16**	16.1847088	8.53309E-08	16.1842488	**2.8422E-05**
7	**21**	21.0256728	1.91473E-08	21.0256137	**2.8116E-06**
8	**22**	19.5391114	3.75425E-08	19.5389739	**7.0395E-06**
9	**24**	14.848343	7.62552E-08	14.8478636	**3.2289E-05**
10	**25**	9.26298748	9.31152E-08	9.26187377	**1.2023E-04**
11	**26**	1.88197455	1.01771E-07	1.87912699	**1.5131E-03**

Fig. 5. Results of the reliability analysis of the WSN in the case study with a) the results regarding the measurement accurcy due to signal attenuation and b) the results regarding the hardware reliability under cyclic loads.

Besides the accuracy, the hardware reliability is calculated and plotted in Figure 5(b). For the calculation, it is assumed that the strains from the FEM model have the value of the strain amplitude for cyclic loads. As one can see, there are regions with a very high reliability over time (stays near $R(t) = 100\ \%$,) in the plot. These are region 6, 9, 10 and 11 close to the free end of the wing box, which have the highest mechanical reliability, but the worst accuracy. This is due to the fact, that the sensor nodes 16, 24, 25 and 26 are positioned where the strains are minimal for the upper surface of the wing box. Therefore, the strain amplitude is the lowest, leading to low loads and therefore higher mechanical lifetimes and the sensor nodes at these positions theoretically could endure an infinite number of cycles. On the other hand, the accuracy is lower than in other regions due to the same reason. The low strain amplitude makes it difficult to distinguish the strain signal from the measurement noise, which leads to a bad SNR. Besides, the transmission distance is longer than for the other nodes, leading to a higher signal attenuation. Therefore, the accuracy is comparatively low for these nodes and regions. In contrast, the regions 1, 2, 7 and 8 have the lowest reliability over time, since these regions are built up by the sensor nodes 11, 12, 21 and 22 close to the clamped end with the highest strain amplitude. However, these regions have the lowest measurement error due to good SNR and short transmission distances to the sink node nearby.

In the plot of mechanical reliability in Figure 5(b), region 5 (sensor node 15) is conspicuous due to its comparatively high reliability over time, even though the region has no redundant measuring sensors. This is due to its position close to a stiffening element inside the wing box, leading to lower strain amplitudes. Interestingly, region 9 (sensor node 24) is positioned close by but has a very much higher reliability because it is positioned a little closer to the stiffening element, leading to a much lower strain amplitude. Since the mechanical reliability of region 5 is comparatively good and the accuracy is pretty low, too, the development engineer of the WSN could assume that this a very good position for the sensor node from a reliability point of view in contrast to region 9, when the data and mechanical point of view are considered.

Especially at the beginning of the plot in Figure 5(b), region 3 shows a good reliability which intersects with the reliability curve of region 5 at around $1.6 \cdot 10^9$ cycles. The higher reliability before the intersection point, even though the sensor nodes 13 and 23 in region 3 are loaded by higher strain amplitudes than sensor node 15, results from the measurement redundancy of sensor node 13 and 23. As shown in Figure 6, sensor node 13 would have a reliability only slightly higher than sensor node 22 in region 8, but with the redundantly measuring sensor node 23, the regions reliability is increased significantly. Besides, both sensor nodes in region 3 have only a low percentage error (see Figure 5(a)), since they are positioned close to the sink node at the area of higher strains and therefore better SNR. This shows the potential of measurement redundancies to increase the mechanical reliability at higher loaded measurement regions, which have on the other hand a higher reliability from a data perspective regarding the accuracy.

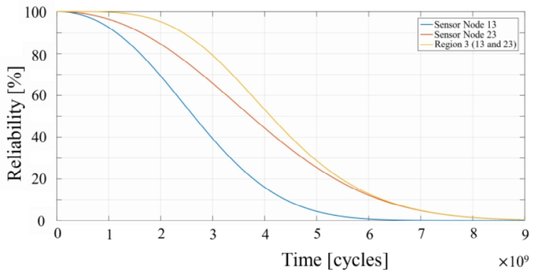

Fig. 6. Comparison of the hardware reliability of the sensor nodes 13 and 23 alone and as parallel order in a region due to redundant measurements.

The comparison of the hardware reliability with the data accuracy in Figure 5 shows a conflict of goals for the WSN. Whilst the reliability of the hardware is comparatively low, the accuracy is maximal for all regions in the WSN. This is due to the fact that high strain amplitudes allow to distinguish the strain signal very well from the noise in the signal transmitted and received. Therefore, if the development engineer of the wing box has to position sensors in the regions 1 and 2, the reliability analysis could show that a higher number of sensor nodes would increase the hardware reliability due to redundancies whilst the accuracy shows that data acquired at these positions is of good quality.

However, all of the regions show a very good accuracy regarding the percentage error, which results from the low transmission ranges. The results would be different, if the transmission range was not in the range of a few meters. This however, would be a use-case in the field of civil engineering and not the here considered mechanical and aerospace engineering. But it becomes clear from the results, that the tradeoff between high signal quality and measurement accuracy to high mechanical lifetime has to be considered when a component-integrated WSN is designed. For this purpose, the presented approach could help development engineers to choose suitable sensor node positions and numbers to deal with this conflict of objectives.

5. Conclusion and future work

The use of wireless sensor networks (WSNs) enables the online and near-real time monitoring of large-scale components. Acquired monitoring data is particularly valuable for product development, especially when optimizing the next product generation concerning loads during the product use-phase. Especially when composite product components are considered, the integration of the WSN directly into the layup enables robust measurements at the inside of the material. However, this integration makes the optimal sensor placement with focus on the system reliability of the WSN very important, since the positions could not be changed after manufacturing and the WSN is not repairable. In a previous study, an automated approach for analyzing the system reliability with focus on the reliability of data transmission along data paths was presented and enhanced in this paper. To achieve this, an in-house developed algorithm for region analysis was applied and most importantly, the accuracy of measured and transmitted data is added to the analysis. This accuracy analysis is based on the calculation of the signal-to-noise ratio (SNR) before and after data transmission, utilizing signal attenuation due to interactions with atmospheric gases. With use of the data accuracy as a second metric, the product developer can consider the hardware reliability as a constraint for data transmission as well as the accuracy as reliability metric to have a hardware and a data-oriented perspective combined in the reliability analysis. The presented approach is tested in an exemplary case study involving a clamped aluminum wing box of an airplane with a WSN comprising 12 sensor nodes and one sink node. In this case study, the applicability was demonstrated, and the advantages for the product developer to find possible weaknesses of the WSN regarding reliable data acquisition were underlined.

In future works, the developed approach should be enhanced further, regarding a more holistic approach on the data side of the WSN reliability. Therefore, the problem of data loss could be integrated to model the reliability of transmission links between the sensor nodes. Additionally, the energetic point of view on the WSN system reliability should be included in the holistic approach incorporating models of battery discharge and energy harvesting. In the context of hardware reliability, the presented approach has the potential to be further enhanced regarding the differentiation of repairable and non-repairable components of the sensor nodes. For example, it may be considered to integrate sensors into the composite layup while locating A/D converters and microprocessors on the surface of a component, allowing these components to be modeled as repairable.

Furthermore, future works should consider changing environmental conditions and not only one condition at a test bench, so that actual operating conditions of e. g. an aircraft could be considered. The very much lower temperature, pressure and vapor density at higher altitudes might lead to fewer signal attenuation since e. g. a higher vapor density leads to higher signal attenuation and the density significantly decreases with increasing altitude. Besides, the accuracy should be enhanced by taking other factors like signal drift over time into account. Therefore, the accuracy should be analyzed over time in use, as the mechanical reliability is. Also, the integration of other failure mechanisms besides fatigue and the calculation using the Wöhler line should be integrated into the methodology to draw a more complete picture on the reliability of the sensor nodes from a hardware point of view.

References

Akyildiz, I.F., Su, W., Sankarasubramaniam, Y. and Cayirci, E. 2002, A survey on sensor networks, IEEE Communications Magazine 40(8), 102–114. https://doi.org/10.1109/MCOM.2002.1024422.

Bertsche, B. 2008, Reliability in Automotive and Mechanical Engineering: Determination of Component and System Reliability, VDI-Buch, 1st ed. 2008, Springer Berlin Heidelberg; Imprint: Springer, Berlin, Heidelberg.

Dâmaso, A., Rosa, N., Maciel, P. 2014, Reliability of wireless sensor networks, Sensors (Basel, Switzerland) 14(9), 15760–15785. https://doi.org/10.3390/s140915760.

Damm, A.M., Spitzmüller, C., Raichle, A.T.S., Bühler, A., Weißgraeber, P. Middendorf, P. 2020, Deep learning for impact detection in composite plates with sparsely integrated sensors, Smart Materials and Structures 29(12), 125014. https://doi.org/10.1088/1361-665X/abb644.

Deif, D., Gadallah, Y. 2017, A comprehensive wireless sensor network reliability metric for critical Internet of Things applications, EURASIP Journal on Wireless Communications and Networking 2017(1), 1–18. https://doi.org/10.1186/s13638-017-0930-3.

Giannetti, F., Reggiannini, R., Moretti, M., Adirosi, E., Baldini, L., Facheris, L., Antonini, A., Melani, S., Bacci, G., Petrolino, A., Vaccaro, A. 2017, Real-Time Rain Rate Evaluation via Satellite Downlink Signal Attenuation Measurement, Sensors 17(8), 1864. https://doi.org/10.3390/s17081864.

Ibrahim, H., Mostafa, N., Halawa, H., Elsalamouny, M., Daoud, R., Amer, H., Adel, Y., Shaarawi, A., Khattab, A., ElSayed, H. 2019, A layered IoT architecture for greenhouse monitoring and remote control, SN Applied Sciences 1(3). https://doi.org/10.1007/s42452-019-0227-8.

Innocent, M.T., Zhang, Z., Boland, C.S., Cao, R., Hu, Z., Geng, Y., Zhai, G., Liu, F., Dai, H., Chen, Z., Zhang, Z., Xiang, H., Zhu, M. 2022. Electromechanical Properties and Resistance Signal Fatigue of Piezoresistive Fiber-Based Strain Gauges, ACS Applied Polymer Materials 4(11), 8335–8343. https://doi.org/10.1021/acsapm.2c01292.

ITU. 2013, RECOMMENDATION ITU-R P.676-9 - Attenuation by atmospheric gases, 09/2013. https://doi.org/.

Keil, S. 2017, Dehnungsmessstreifen, SpringerLink Bücher, 2. Aufl. 2017, Springer Vieweg, Wiesbaden.

Lachmayer, R., Mozgova, I., Reimche, W., Colditz, F., Mroz, G., Gottwald, P. 2014, Technical Inheritance: A Concept to Adapt the Evolution of Nature to Product Engineering, Procedia Technology 15, 178–187. https://doi.org/10.1016/j.protcy.2014.09.070.

Lachmayer, R., Mozgova, I., Scheidel, W. 2016, An Approach to Describe Gentelligent Components in their Life Cycle, Procedia Technology 26, 199–206. https://doi.org/10.1016/j.protcy.2016.08.027.

Lee, H., Tsai, H.-M., Tonguz, O.K. 2009, On the Security of Intra-Car Wireless Sensor Networks, in 2009 IEEE 70th Vehicular Technology Conference Fall, 20.09.2009 - 23.09.2009, Anchorage, AK, USA, IEEE, 1–5.

Lin, C.-M., Teng, H.-K., Yang, C.-C., Weng, H.-L., Chung, M.-C., Chung, C.-C. 2010. A mesh network reliability analysis using reliability block diagram, in 2010 8th IEEE International Conference on Industrial Informatics: (INDIN 2010) ; Osaka, Japan, 13 - 16 July 2010, 7/13/2010 - 7/16/2010, Osaka, Japan, IEEE, Piscataway, NJ, 975–979.

Meyer zu Westerhausen, S., Schneider, J., Lachmayer, R. 2023a. Automatic Reliability Assessment of Data Paths in Component-Integrated Sensor Networks, in Brito, M.P., Aven, T., Baraldi, P., Čepin, M., Zio, E. (Eds.), Proceeding of the 33rd European Safety and Reliability Conference, 03.09.2023 - 07.09.2023, Research Publishing Services, Singapore, 2223–2229.

Meyer zu Westerhausen, S., Schneider, J., Lachmayer, R. 2023b, Reliability Analysis for Sensor Networks and Their Data Acquisition: A Systematic Literature Review, Proceedings of the Design Society 3, 3065–3074. https://doi.org/10.1017/pds.2023.307.

Valoriani, F., Esposito, M., Gherlone, M. 2022, Shape Sensing for an UAV Composite Half-Wing: Numerical Comparison between Modal Method and Ko’s Displacement Theory, Aerospace 9(9), 509. https://doi.org/10.3390/aerospace9090509.

Wang, C., Xing, L., Vokkarane, V.M., Sun, Y. 2014, Reliability and lifetime modeling of wireless sensor nodes, Microelectronics Reliability, 54(1), 160–166. https://doi.org/10.1016/j.microrel.2013.08.001.

Wang, R., Tong, Y., Tian, L., Wang, D. 2021. Reliability Analysis of Different Fault-Tolerant Mechanisms in Wireless Sensor Networks, In Patnaik, S. (Ed.), 2021 3rd International Conference on Applied Machine Learning: ICAML 2021: 23-25 July, Changsha, China proceedings, 7/23/2021 - 7/25/2021, Changsha, China, IEEE, Piscataway, NJ, 250–256.

Welzbacher, P., Geipl, A., Kraus, B., Puchtler, S., Kirchner, E. 2023, A Follow-Up on The Methodical Framework for the Identification, Analysis and Consideration of Uncertainty in the Context of the Integration of Sensory Functions by Means of Sensing Machine Elements, Proceedings of the Design Society 3, 141–150. https://doi.org/10.1017/pds.2023.15.